Journal of Photochemistry and Photobiology A: Chemistry 211 (2010) 74–77

Contents lists available at ScienceDirect

Journal of Photochemistry and Photobiology A: Chemistry

journal homepage: www.elsevier.com/locate/jphotochem

Efficiency of porous silicon photosensitizer in the singlet oxygen-mediated oxidation of organic compounds

Konstantin Loponov[a], Bernhard Goller[b], Andriy Moskalenko[b], Dmitry Kovalev[b,*], Alexei Lapkin[a,*]

[a] School of Engineering, University of Warwick, Library Road, Coventry, UK
[b] Department of Physics, University of Bath, Bath, UK

ARTICLE INFO

Article history:
Received 22 November 2009
Received in revised form 10 February 2010
Accepted 12 February 2010
Available online 19 February 2010

Keywords:
Singlet oxygen
Porous silicon
Photochemistry

ABSTRACT

The efficiency of singlet oxygen photosensitization by porous silicon is compared with that of a conventional dye photosensitizer tetraphenylporphine by means of singlet oxygen-mediated photooxidation of α-terpinene. Based on photoluminescence measurements it was concluded that the efficiency of porous silicon as a sensitizer is much lower than that of the conventional organic dye. The main reasons for this are the low quantum yield of long living photoinduced electronic excitations (excitones) confined in silicon nanocrystals and deactivation of singlet oxygen by H-terminated internal surface of porous silicon powder. Efficient quenching of excitons in porous silicon by 1,3-diphenylisobenzofuran *via* the direct energy transfer was demonstrated. This process is believed to be responsible for photobleaching of 1,3-diphenylisobenzofuran at its millimolar concentrations.

1. Introduction

Chemical reactions mediated by singlet oxygen ($^1O_2$) are of much current interest since $^1O_2$ is involved in numerous processes important in molecular physics, photochemistry, biology and medical sciences [1–5]. One of the key applications of highly reactive $^1O_2$ is in photodynamic therapy of cancer [3]. Applications of singlet oxygen mediated reactions in synthetic chemistry are also of significant interest, see for example review [1]. $^1O_2$ generation in solutions is most frequently done via photosensitized energy transfer from the excited electronic states of different molecules, such as organic dyes, metal–organic complexes, fullerenes to O_2 [6–8]. Conventionally, photosensitized reactions are performed in homogeneous solutions. However, a homogeneous process has some disadvantages with respect to separation of a sensitizer from the reaction mixture, and thus the sensitizer is not reusable, unless it is immobilized [9,10]. It is therefore useful to develop a highly effective heterogeneous photosensitizer system.

Recently, it has been discovered that photoexcited porous silicon (PSi) nanostructures may be used as $^1O_2$ sensitizers [11]. Due to its indirect band gap structure bulk Si is a very poor light emitter. However, at nanoscale, quantum size effects result in the increase in the energy of excitons and also the probability of their radiative recombination. Therefore relatively high photoluminescence (PL) quantum yields can be achieved [12,13]. The indirect band-gap structure of Si nanocrystals is the reason for very slow recombination rate (in the order of 10ths of μs at room temperature). It is also important to mention that statistically 75% of photoexcited excitons persist at room temperature in their triplet states [14,15]. Due to the long lifetime of excitons confined in Si nanocrystals the energy of photons is stored in electronic form and can then be transferred to other substances [16]. Moreover, the band-gap energy of Si nanocrystals can easily be adjusted from the bulk Si band-gap (1.1 eV) up to about 2.5 eV, simply by varying the size of nanocrystals [14]. Therefore, by choosing the proper nanocrystals size, the energy of excitons can be tuned to match the singlet-triplet splitting energy of a certain acceptor, e.g. O_2. A large surface area (up to about 500 $m^2\,g^{-1}$), mesopore-range porous structure (*ca.* 7 nm) [17] and good dispersibility of hydrophobic Si nanocrystals in organic solvents allow good accessibility of the surface of Si nanocrystals for different molecules. It should also be mentioned that contrary to most conventional photosensitizers PSi efficiently absorbs all photons with energies higher than the nanocrystals band-gap. Therefore, a broad range of light sources can be used for excitation.

Excitons photogenerated in PSi were proven to generate $^1O_2$ in gaseous environment, in organic solvents and in water [11,18,19]. 1,3-Diphenylisobenzofuran (DPBF) bleaching in the presence of photoexcited PSi has already been demonstrated, both in a spectroscopic cell and in a recirculating laboratory scale reactor [20,21]. However, in spite of the fact that DPBF easily undergoes a 1,4-cycloaddition reaction with $^1O_2$ (an overall rate constant, $k_R = 9 \times 10^8$ l mole^{-1} s^{-1}) [22], there is a possibility of direct energy

* Corresponding authors. Tel.: +44 02476151101; fax: +44 0247641822.
E-mail addresses: d.kovalev@bath.ac.uk (D. Kovalev), a.lapkin@warwick.ac.uk (A. Lapkin).

1010-6030/$ – see front matter © 2010 Elsevier B.V. All rights reserved.
doi:10.1016/j.jphotochem.2010.02.005

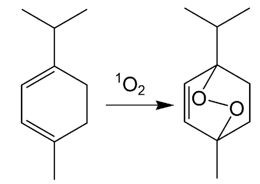

Scheme 1.

transfer from triplet excitons confined in Si nanocrystals to DPBF molecules [16,21]. Contrary to oxidation mediated by photosensitised $^1O_2$ (Type I pathway), this process (Type II pathway) occurs via donation and acceptance of protons or electrons which results in the formation of free radicals or free-radical ions [6,23] and can also lead to degradation of DPBF. Therefore, the data reported earlier leave doubt over the specific mechanism of photobleaching and do not provide direct comparison between the sensitising efficiency of PSi with that of the conventional organic dye sensitizers.

In this study we compare the efficiency of PSi in $^1O_2$ mediated photooxidation of α-terpinene with that of a conventional organic dye photosensitizer tetraphenylporphin (TPP). We used α-terpinene as a $^1O_2$ trap since it easily reacts with $^1O_2$ via 1,4-cycloaddition ($k_R = 10^8\,\mathrm{l\,mole^{-1}\,s^{-1}}$ [24]) producing ascaridol (Scheme 1), and it has low efficiency of quenching of PSi PL. An attempt to clarify the mechanisms which can be involved in the photobleaching of DPBF was also made.

2. Materials and methods

Photooxidation of α-terpinene was carried out in a recirculating laboratory scale reactor described elsewhere [20]. 5.9 ml of α-terpinene and a sensitizer (TPP or PSi, 8.7×10^{-5} M or 0.2 wt.%, respectively) were dissolved/dispersed in 250 ml of dichloromethane. The reaction mixture was saturated by O_2 via gas bubbling. Afterwards, a 75 W Xe short-arc lamp was switched on providing 5 cm long illumination zone within a glass tube having outer diameter of 18 and 1.5 mm thickness of annular reaction space. Aliquots were taken for analysis at different times during the illumination. About 2–3 ml of irradiated reaction mixture was evaporated (PSi powder was filtered prior evaporation). The residue was dissolved in *ca.* 2 ml of chloroform-d for ^{1}H nuclear magnetic resonance (NMR) analysis. Temperature of the reaction mixture was kept at 20 °C and liquid flow rate was 40 ml min^{-1}.

PSi powder was prepared from metallurgical grade polycrystalline Si powder (mean particle size of 4 μm) [25]. The powder was first immersed in a solution of HF and water to remove surface SiO_2 layer, then HNO_3 was added gradually until the ratio of used chemicals was about 4:1:20 of HF:HNO_3:H_2O. The etching was finished when an efficient red-orange emission under illumination by ultraviolet light appeared. According to high resolution transmission electron microscopy images the size of Si nanocrystals comprising the PSi powder particles was in the range of 3–7 nm. The average pore diameter of about 7 nm was calculated from the low temperature nitrogen adsorption data using the Barrett–Joyner–Halenda model [17].

In PL spectroscopy experiments, 30 mg of PSi powder (or 37 μM of TPP) were dispersed in 2 ml of solvent (DCM, C_6F_6 or CCl_4) and different amounts of α-terpinene were added in different experiments as detailed in Section 3. PL was excited by an Ar^+ laser (energy 2.54 eV) with an excitation intensity of up to 500 mW cm^{-2}. Near-infrared PL measurements aiming for detection of radiative relaxation of $^1O_2$ ($^1\Delta$–$^3\Sigma$ transition) were performed in O_2-saturated solvents using an InGaAs array detector coupled with a single monochromator. For measurements in the visible range a Si charge-coupled device was used. All optical spectra were corrected to the sensitivity of the respective optical setup.

3. Results and discussion

3.1. Photooxidation of α-terpinene

From the NMR spectra obtained in the experiment with the conventional triplet dye $^1O_2$ sensitizer TPP in the recirculating photochemical reactor it was found that 15% conversion of α-terpinene to ascaridol was achieved after 3.5 h of illumination. In the case of the PSi sensitizer formation of ascaridol was not detected even after illumination for 24 h. However, this does not mean that reaction does not take place at all, rather a more sensitive method of detection is required, for example, the direct measurement of $^1O_2$ PL by near infrared spectroscopy, described below. Another potential explanation of the lack of ascaridol signal in NMR spectra is the feasibility of its sorption on the extended surface area of solid PSi, especially as the reaction is very slow in the case of this sensitizer and the expected product concentrations are very small.

In general, the rate of photooxidation depends on the bimolecular rate constant and on the $^1O_2$ steady-state concentration in solution [6,8]. In equilibrium the rate of $^1O_2$ generation, ϕI_a equals the rate of its decay $k_D[^1O_2]_{SS}$ and therefore steady-state concentration of $^1O_2$ is:

$$[^1O_2]_{SS} = \frac{\phi I_a}{k_D} \qquad (1)$$

Here ϕ is quantum yield of $^1O_2$ generation, I_a is the intensity of the absorbed light and k_D is the first order $^1O_2$ decay constant. In the presence of $^1O_2$ quencher *R*, steady-state concentration of $^1O_2$ is reduced:

$$[^1O_2]_{SS} = \frac{\phi I_a}{(k_D + k_R[R])} \qquad (2)$$

Here k_R is an overall rate constant for physical quenching and chemical reaction with $^1O_2$. Reduction in the steady-state concentration of $^1O_2$ in a solution can be detected as the decrease of $^1O_2$ PL emission intensity at 1270 nm (0.98 eV). Therefore, using more sensitive PL spectroscopy it is possible to monitor the photooxidation of α-terpinene and compare the efficiencies of both sensitizers.

Measuring the intensity of $^1O_2$ PL during gradual addition of small amounts of α-terpinene to the suspensions of PSi (0.9 wt.% in C_6F_6) we found that 460 μM concentration of α-terpinene is sufficient to suppress $^1O_2$ PL almost completely (Fig. 1). A decrease in $^1O_2$ PL (or, respectively, of $^1O_2$ steady-state concentration) can take

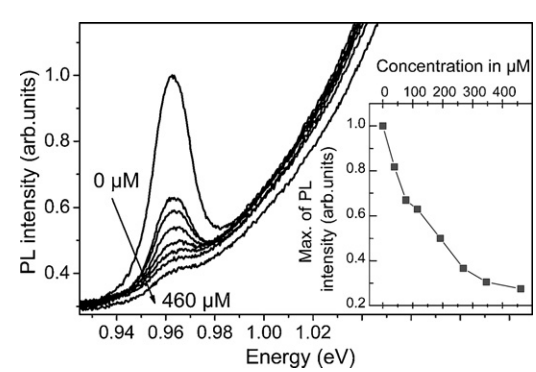

Fig. 1. PL spectra of $^1O_2$ ($^1\Delta$–$^3\Sigma$ decay transition) photogenerated by 0.9 wt.% of PSi powder in C_6F_6. α-Terpinene was gradually added to the solution to obtain the following concentrations, from top to bottom: 0, 40, 75, 120, 200, 270, 350, 460 μM. Inset: evolution of the maximum of the $^1O_2$ luminescence versus α-terpinene concentration. The broad PL from PSi dangling bonds is subtracted in order to estimate the PL intensity of the $^1O_2$ emission line. $I_{ex.} = 30\,\mathrm{mW\,cm^{-2}}$, $E_{ex.} = 2.54$ eV.

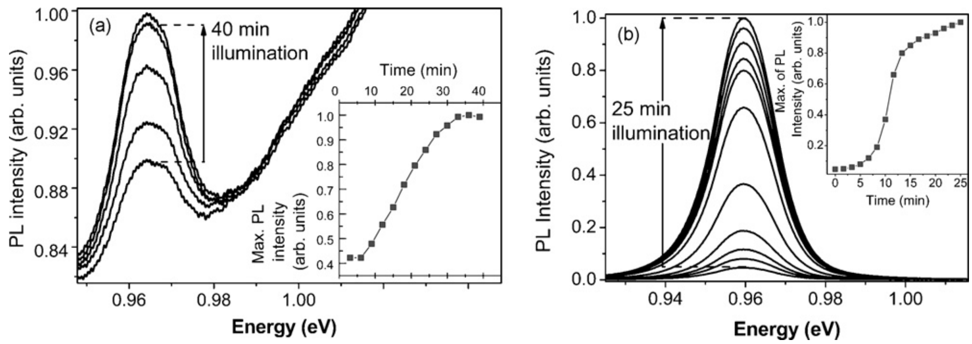

Fig. 2. Time evolution of the $^1O_2$ PL spectra ($^1\Delta$–$^3\Sigma$ decay transition) after initial addition of (a) 75 μM α-terpinene to 0.9 wt.% of PSi powder in C_6F_6, $I_{ex.}$ = 500 mW cm^{-2}, $E_{ex.}$ = 2.54 eV; (b) 30 mM of α-terpinene to 37 μM TPP in C_6F_6, $I_{ex.}$ = 15 mW cm^{-2}, $E_{ex.}$ = 2.54 eV. Insets: $^1O_2$ PL peak intensity as a function of time for the respective images. In the case of PSi the broad PL from Si defects was subtracted in order to estimate the PL intensity.

place either due to physical quenching or chemical reaction [7]. In the case of the physical quenching, addition of a specific amount of quencher will result in the corresponding constant level of PL suppression. On the contrary, if chemical reaction path dominates, concentration of the reagent decreases with time, and consequently the level of $^1O_2$ PL quenching should be reduced. The corresponding experiment has been done as seen in Fig. 2.

Following the initial quenching of $^1O_2$ PL with 75 μM of α-terpinene, the PL intensity recovered almost completely over 40 min of illumination by an Ar$^+$ laser (500 mW cm^{-2} illumination intensity). This indicates a chemical reaction between $^1O_2$ and α-terpinene. In Fig. 2a the PL signal without α-terpinene corresponds to the curve having the largest intensity, whereas the curve with the lowest intensity is recorded immediately after the addition of the reactant. The lines between these two limits from bottom to the top clearly show recovery of $^1O_2$ luminescence after continuous illumination for 12, 21 and 40 min, respectively. This is easily seen in the inset in Fig. 2a showing the intensity of the $^1O_2$ PL as a function of time.

The corresponding experiment with a conventional sensitizer TPP is shown in Fig. 2b. A similar ratio of sensitizer to the reactant molecules was used (37 μM in C_6F_6). To estimate the amount of TPP we assumed that PSi is composed from nanocrystals with an average size of 5 nm acting as elementary absorbers. As in the case of the PSi sensitizer, initial addition of α-terpinene (30 mM concentration) leads to nearly complete suppression of $^1O_2$ PL. However, in the case of the TPP sensitizer, complete conversion of α-terpinene occurred over 25 min using a much lower light intensity (15 mW cm^{-2}).

3.2. Efficiency of $^1O_2$ generation by PSi and TPP sensitizers

The overall $^1O_2$ generation rate mediated by PSi is a product of the absorbed light intensity, the quantum yield of photogenerated long living excitons and the efficiency of energy transfer from photoexcited Si nanocrystals to O_2. Despite the high efficiency of the latter process, which is about 80% [19], the $^1O_2$ generation efficiency cannot exceed 0.05-0.1, because quantum yield of PSi PL (or the number of long living excitons created by light per number of absorbed photons) does not exceed this value [14]. Therefore, in the case of the PSi sensitizer the illumination time or intensity of light should be significantly increased to achieve the same conversion of α-terpinene to ascaridol as with TPP, having quantum yield of $^1O_2$ generation in the range of about 0.7–0.9 [6].

We also directly compared the efficiencies of $^1O_2$ formation by both PSi and TPP. Fig. 3 shows that under similar illumination conditions and with a similar amount of primary absorbers in the reaction system the intensity of the emission peak from the $^1\Delta$–$^3\Sigma$ transition of $^1O_2$ generated by TPP (and, therefore, $^1O_2$ steady-state concentration) is over 200 times higher than the corresponding values achieved using PSi. This is likely to be specific to the particular sample of porous silicon and may vary between samples. The discrepancy between the observed $^1O_2$ steady-state concentrations generated by TPP and PSi photosensitizers (Fig. 3) and the corresponding quantum yields of $^1O_2$ formation indicates that there are additional decay channels for $^1O_2$ in PSi, which are discussed below.

As it was mentioned earlier, steady-state concentration of $^1O_2$ in the absence of added quenchers can be expressed by Eq. (1). If TPP is used as $^1O_2$ sensitizer, the $^1O_2$ decays mostly due to collisions with molecules of solvent, and therefore, decay constant k_D is determined only by lifetime of $^1O_2$ in a particular solvent, τ_d. In the case of PSi an additional term, given by the deactivation time of $^1O_2$ by the surface of Si nanocrystals, τ_q, contributes to the solvent-mediated quenching of $^1O_2$. It should be noted that the surface of Si nanocrystals is H-terminated and, due to high frequency of Si–H bonds oscillations, this surface can very efficiently quench $^1O_2$ molecules during collisions [7]. The total lifetime of $^1O_2$, τ_D, measured in suspensions of PSi (1 wt.%) in C_6F_6 in the absence of other quenchers was found to be 3.9 ms [21]. Taking into account this value and the lifetime of $^1O_2$ in pure C_6F_6 (τ_d = 25 ms [26]) it is possible to estimate the deactivation time of $^1O_2$ by the surface of Si nanocrystals, using Eq. (3):

$$\frac{1}{\tau_D} = \frac{1}{\tau_d} + \frac{1}{\tau_q} \tag{3}$$

Based on this equation τ_q was estimated to be about 4.9 ms. This value implies that 84% of photogenerated $^1O_2$ is deactivated in PSi due to collisions with its hydrogenated internal surface.

Apart from quenching of excitons confined in Si nanocrystals by O_2, another possible deactivation pathway is direct quenching

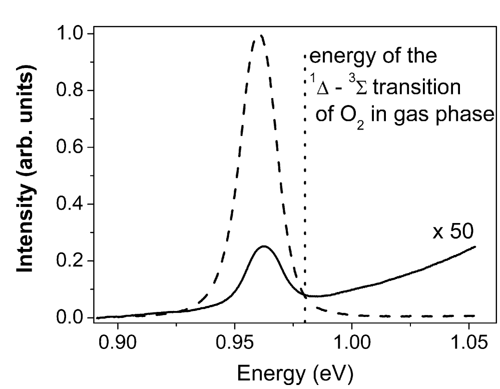

Fig. 3. PL spectra of $^1O_2$ ($^1\Delta$–$^3\Sigma$ decay transition) generated by 0.9 wt.% of PSi in CCl_4 (solid line) and 37 μM TPP (dashed line). Solid curve was multiplied by a factor of 50. Dotted vertical line indicates the energy of $^1O_2$ $^1\Delta$–$^3\Sigma$ transition in the gas phase. $I_{ex.}$ = 15 mW cm^{-2}, $E_{ex.}$ = 2.54 eV.

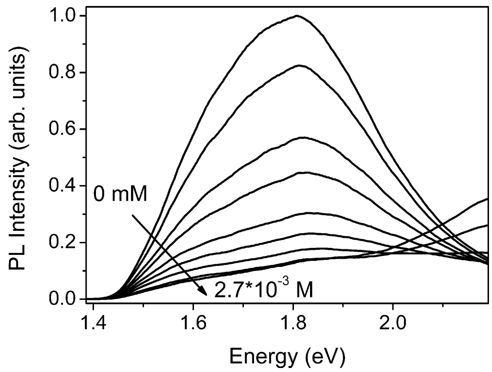

Fig. 4. PL spectra of 0.9 wt.% PSi powder dispersed in DCM containing various concentrations of DPBF, from top to bottom: 0, 35, 70, 100, 210, 350, 700 μM, 1.7, 2.7 mM Note, at high concentrations of DPBF its PL can be clearly seen in the spectral range at higher energies. $E_{ex.}$ = 2.54 eV, $I_{ex.}$ = 500 μW cm^{-2}.

of excitons by organic molecules [16]. Investigating the quenching of PL from PSi (suspensions of 1.1 wt.% in DCM) using gradual addition of α-terpinene, or earlier studied DPBF, it was found that DPBF significantly suppresses PSi PL even in micromolar concentrations. About 0.7 mM was sufficient to quench all photoexcited excitons (see Fig. 4). Since the triplet state energy of DPBF lies about 1.48 eV above the ground state and almost all photoexcited excitons in Si nanocrystals have energies above this value, this process is favorable [27].

For the larger DPBF concentrations (about 0.8 mM) the increase of PL intensity for the high energy side of the spectral range is caused by DPBF luminescence. At high concentrations it absorbs laser light efficiently and, therefore, luminesces stronger than PSi. In contrast, α-terpinene does not quench PSi PL even at 2 M concentrations. PSi PL quenching means that if the mM concentrations of DPBF are used in photobleaching experiments (see [20]), energy of almost all excitons is directly transferred to DPBF molecules. This process restricts formation of $^1O_2$ and the photobleaching of DPBF mainly takes place via a Type II pathway described above.

4. Conclusions

An extensive comparative study of the photosensitizing efficiency of a proposed photosensitizer based on PSi and a conventional dye sensitizer TPP was performed. By monitoring the PL emission line of $^1O_2$ we concluded that the photosensitizing efficiency of PSi is much lower than that of TPP. We attributed this effect mainly to the low quantum yield of PSi PL (in the order of the few percents) and to very efficient energy transfer from electronically excited $^1O_2$ molecules to high frequency surface Si–H vibration modes which is crucial for deactivation of $^1O_2$ states. Furthermore, we believe that direct energy transfer from photoexcited excitons in PSi to DPBF molecules at millimolar concentrations is responsible for DPBF photobleaching

Acknowledgements

The authors are grateful for useful technical advice and fruitful scientific discussions with Dr. G. Aliev and Mr. S. Polisski. This work was supported in part by EPSRC (Project EP/E012183/1), US Army research grant (W911NF0820011) and Vesta Ceramics.

References

[1] M.C. DeRosa, R.J. Crutchley, Photosensitized singlet oxygen and its applications, Coord. Chem. Rev. 233/234 (2002) 351–357.
[2] D.L. Gilbert, C.A. Colton, Reactive Oxygen Species in Biological System: An Interdisciplinary Approach, Plenum, New York, 1999.
[3] J.G. Moser, Photodynamic Tumor Therapy: 2nd and 3rd Generation Photosensitizers, Gordon and Breach, London, 1998.
[4] I.E. Kochevar, M.C. Lynch, S. Zhuang, C.R. Lambert, Singlet oxygen, but not oxidizing radicals, induces apoptosis in HL-60 cells, Photochem. Photobiol. 72 (2000) 548–553.
[5] T. Maisch, J. Baier, B. Franz, M. Maier, M. Landthaler, R. Szeimies, W. Baumler, The role of singlet oxygen and oxygen concentration in photodynamic inactivation of bacteria, PNAS 104 (2007) 7223–7228.
[6] F. Wilkinson, W.P. Helman, A.B. Ross, Quantum yields for the photosensitized formation of the lowest electronically excited singlet state of molecular oxygen in solution, J. Phys. Chem. Ref. Data 22 (1993) 113–262.
[7] C. Schweitzer, R. Schmidt, Physical mechanisms of generation and deactivation of singlet oxygen, Chem. Rev. 103 (2003) 1685–1757.
[8] F. Wilkinson, W.P. Helman, A.B. Ross, Rate constants for the decay and reactions of the lowest electronically excited singlet state of molecular oxygen in solution. An expanded and revised compilation, J. Phys. Chem. Ref. Data 24 (1995) 663–1021.
[9] A.P. Schaap, A.L. Thayer, E.C. Blossey, D.C. Neckers, Polymer-based sensitizers for photooxidations, J. Am. Chem. Soc. 97 (1975) 3741–3745.
[10] R. Sasai, D. Sugiyama, S. Takahashi, Z. Tong, T. Shichi, H. Itoh, K. Takagi, The removal and photodecomposition of *n*-nonylphenol using hydrophobic clay incorporated with copper–phthalocyanine in aqueous media, J. Photochem. Photobiol. A: Chem. 155 (2003) 223–229.
[11] D. Kovalev, E. Gross, N. Künzner, F. Koch, V.Yu. Timoshenko, M. Fujii, Efficient resonant energy transfer from excitons confined in silicon nanocrystals to molecular oxygen, Phys. Rev. Lett. 89 (2002) 1–4, 37401.
[12] V. Lehmann, U. Gösele, Porous silicon formation: a quantum wire effect, Appl. Phys. Lett. 58 (1991) 856–858.
[13] D. Kovalev, H. Heckler, M. Ben-Chorin, G. Polisski, M. Schwartzkopff, F. Koch, Breakdown of the *k*-conservation rule in Si nanocrystals, Phys. Rev. Lett. 81 (1998) 2803–2806.
[14] D. Kovalev, H. Heckler, G. Polisski, F. Koch, Optical properties of silicon nanocrystals, Phys. Status Solidi B 215 (1999) 871–932.
[15] A.G. Cullis, L.T. Canham, P.D.J. Calcott, The structural and luminescence properties of porous silicon, J. Appl. Phys. 82 (1997) 909–965.
[16] B. Goller, S. Polisski, D. Kovalev, Spin-flip excitation of molecules mediated by photoexcited silicon nanocrystalls, Phys. Rev. B 75 (2007) 1–4, 073403.
[17] S. Polisski, B. Goller, A. Lapkin, S. Fairclough, D. Kovalev, Synthesis and catalytic activity of hybrid metal/silicon nanocomposites, Phys. Status Solidi (RRL) (2008) 132–134, 2:3.
[18] M. Fujii, S. Minobe, M. Usui, S. Hayashi, E. Gross, J. Diener, D. Kovalev, Generation of singlet oxygen at room temperature mediated by energy transfer from photoexcited porous Si, Phys. Rev. B 70 (2004) 1–5, 085311.
[19] M. Fujii, D. Kovalev, B. Goller, S. Minobe, S. Hayashi, V.Y. Timoshenko, Time-resolved photoluminescence studies of the energy transfer from excitons confined in Si nanocrystals to oxygen molecules, Phys. Rev. B 72 (2005) 1–8, 165321.
[20] A.A. Lapkin, V. Boddu, G.N. Aliev, B. Goller, S. Polisski, D. Kovalev, Photooxidation by singlet oxygen generated on nanoporous silicon in a LED-powered reactor, Chem. Eng. J. 136 (2008) 331–336.
[21] M. Fujii, M. Usui, S. Hayashi, E. Gross, D. Kovalev, N. Kunzner, J. Diener, V.Y. Timoshenko, Chemical reaction mediated by excited states of Si nanocrystals-singlet oxygen formation in solution, J. Appl. Phys. 95 (2004) 3689–3693.
[22] I.B.C. Matheson, D.A. Lightner, Oxodipyrromethenes as reactive singlet oxygen acceptors. Measurement of their chemical reaction rates by a laser flash photolysis technique, Photochem. Photobiol. 29 (1979) 933–935.
[23] C.S. Foote, Mechanisms of photosensitized oxidation, Science 162 (1968) 963–970.
[24] B.M. Monroe, Rate constants for the reaction of singlet oxygen with conjugated dienes, J. Am. Chem. Soc. 103 (1981) 7253–7256.
[25] S. Limaye, S. Subramanian, B. Goller, J. Diener, D. Kovalev, Scaleable synthesis route for silicon nanocrystal assemblies, Phys. Status Solidi A 204 (2007) 1297–1301.
[26] R. Schmidt, The influence of heavy atoms on the deactivation of singlet oxygen (delta) in solution, J. Am. Chem. Soc. 111 (1989) 6983–6987.
[27] W.G. Herkstroeter, P.B. Merkel, The triplet state energies of rubrene and diphenylisobenzofuran, J. Photochem. 16 (1981) 331–342.